PCCP

Accepted Manuscript

ROYAL SOCIETY OF CHEMISTRY

www.rsc.org/pccp

Journal Name

COMMUNICATION

Fractional Photo-Current Dependence of Graphene Quantum Dots Prepared from Carbon Nanotubes

Received 00th January 20xx,
Accepted 00th January 20xx

DOI: 10.1039/x0xx00000x

www.rsc.org/

Sumana Kundu,[a,c] Sujoy Ghosh,[b] Michael Fralaide,[b] T.N.Narayanan,[d] Vijayamohanan K. Pillai[a,c,e] and Saikat Talapatra[b*]*

We report on the photo-conductivity studies of chemically synthesized Graphene quantum dots (GQDs) of average size 12 nm obtained by the oxidative acid treatment of MWCNTs. The dependence of photocurrent I_{ph} ($I_{ph} = I_{ill} - I_{dark}$) on laser intensity P under a wide range of laser intensities (5mW ≤ P ≤ 60 mW) shows a fractional power dependence of I_{ph} on light intensity. The temperature dependence (300 K < T < 50 K) of I_{ph} observed in thin films of these GQDs, indicates that in the higher temperature region (T > ~ 100 K) as the temperature increases the number of thermally generated carriers increase resulting in increased I_{ph}. At sufficiently low temperatures (T ≤ 100 K), a constant I_{ph} is observed, indicating a constant photo carrier density. Such a behavior is typically observed in many photoactive disordered semiconductors, which are often used in a variety of applications. We believe that the investigations presented here will enhance our understanding of photo phenomenon in chemically obtained GQDs.

The presence of inherent zero bandgap in graphene, to a large extent, poses a severe barrier in developing graphene based materials for a number of niche electronic applications. As such, band gap engineering of these materials is crucial for achieving technological breakthroughs related to carbon based nano-opto electronics. Band gap engineering in graphene can be performed using several techniques such as, by reducing the size of graphene to nano scale regions having one or a few number of layers, and by doping with external elements. Quantum confinement can easily be introduced to a pristine zero band gap graphene lattice which has an exciton-Bohr radius of infinity.[1] Thus the so called three dimensionally quantum confined graphene arise with a certain band gap. It can be tuned from a semiconductor to an insulator, by simply manipulating the band gap. For example, recent density functional theory calculations show that a maximum of up to 7 eV of band gap can be achieved from the smallest possible graphene quantum dot (GQDs) which is supposed to be a benzene like structure.[2] Such flexibility in the band gap engineering as well as good optical absorption has made these materials very attractive for optical and optoelectronic applications.[3,4] By virtue of the quantum confinement, GQDs show fluorescence and single electron transfer[5] properties which can be observed more clearly in ultra-small (3 nm) GQDs. However, poor quantum yield limits the performance of GQDs in some potential optical applications which can be avoided by encapsulating GQDs with some organic ligands or doping to enhance the quantum yield. There are several routes to synthesize pristine GQDs, doped GQDs as well as ligand modified GQDs[6,7,2] such as electron beam lithography, acidic exfoliation, electrochemical oxidation, microwave-assisted hydrothermal synthesis, plasma jet and oxidative treatment of coal[8] and so on and they come under the popular top down method. Recent reports say that thermal plasma jet[9] can produce bulk quantities of GQDs and similarly microwave treatment of graphite to GQDs in presence of $KMnO_4$ in acidic condition will also lead to bulk GQD production.[10] Bottom-up routes include building up of molecular species often in solution or gas phase using different chemistries like cyclo-dehydrogenation of polyphenylene precursors, carbonization or fragmentation of special organic precursors (for example, C_{60} etc). The bottom-up methods have some privileges on the top down methods in terms of rendering exciting opportunities to precisely control many important parameters of GQDs like size, shape, edge states etc. which in turn control their properties.[11,2] But, these methods always suffer from major drawbacks which involve complex synthetic procedures, and sometimes the special organic precursors may be too difficult to be obtained in high purity form. The physical properties of GQDs are highly dominated by the route followed for their synthesis, indicating the role of chemical structure, morphology, and nature of defects in determining the resultant carrier transport in GQDs. Starting materials too play an important role in the synthesis of GQDs. Commonly used starting

[a] *CSIR-Central Electrochemical Research Institute (CSIR-CECRI), Karaikudi-630006, India.*
[b] *Department of Physics, Southern Illinois University, Carbondale, IL-62901, USA.*
[c] *Academy of Scientific & Innovative Research, Chennai,600113, India.*
[d] *TIFR-Centre for Interdisciplinary Sciences, Tata Institute of Fundamental Research, Hyderabad-500 075, India.*
[e] *CSIR-National Chemical Laboratory (CSIR-NCL), Pune-411008 MH, India.*
Electronic Supplementary Information (ESI) available: [Experimental detail]. See DOI: 10.1039/x0xx00000x

materials are graphite,[10] MWCNTs,[5,6] carbon nano-fibers[7] etc. However reports are available for GQDs production from some unconventional sources like coal,[8] glucose etc. Due to its amazing properties and low cytotoxicity, applications of GQDs stroll a domain from biomedical engineering to photovoltaic.[11-15] Regarding some optical applications of GQDs there are few reports on the measurements of photo response with temperature and current-voltage (I-V) measurements using back gate voltage for photodetectors,[16] and light emitting diode.[3] There are several other reports on graphene based photodetectors or some coupled graphene system with conventional QDs.[16-19]

Here we aim to investigate fundamental optical properties of GQDs synthesized from Multi walled Carbon Nanotubes through photoconductive studies. MWCNTs have been used as the starting material due to their better reactivity owing to their strained structure compared to flat sheet like stable graphite entity which finally leads to less reaction time compared to that of graphite. Here, these GQDs are small fragment of graphene entities (average 12 nm size) enriched with some -COOH and -OH functional groups due to acidic oxidation of the precursor material. We have performed a laser power and temperature dependent photo response studies to unravel the photocurrent behavior of GQDs. Thin film GQD devices were fabricated on pre-patterned electrodes for photoconduction measurement. A non-linear dependence of I_{ph} on light intensity was observed. We found that I_{ph} shows a power dependence behavior $I_{ph} \sim P^{\gamma}$. Further, temperature dependence of photocurrent in GQD thin films show the disordered nature of these films.These results are compared and discussed in the light of earlier report on photo response of GQDs like moiety applying back gate voltage.[16]

GQDs were synthesized by chemical oxidation of MWCNTs and the resultant GQDs have an average size of ~ 12 nm (schematic Figure 1). Figure 2(a) is the TEM image of GQDs which exhibits an average particle size of 12 nm with a particle size distribution width of 10-15 nm as shown in the inset. Figure S1 (a) represents the enlarged TEM image for clarity while the HRTEM image has been shown in Figure S1 (b). This image shows the clear lattice fringes with a d spacing of 0.34 nm corresponding to (002) plane of graphite which matches well with the XRD pattern of the GQDs provided in Figure S1 (c) with a d value of 0.35 nm. Figure S1 (d) reveals the AFM image of the GQDs with a height profile showing the maximum height of 1.5 nm indicating 2 to 3 layers of graphene layers in the GQDs. Figure 2(b) is a UV-VIS spectrum of GQDs suspended in water which shows a broad absorption peak at 240 nm due to $\pi \rightarrow \pi^*$electronic transitions as is well reported for π electron systems. Photoluminescence studies were conducted using a fluorimeter and the excitation was kept at 370 nm, an intense emission spectrum is observed at around 450 nm (Fig 2(c)) and the inset image shows the green emission from the GQDs suspension (in water, water is kept as a control in the left side) when exposed to a UV lamp.

Micro-Raman spectrum of GQDs is shown in Fig 2(d). A strong D line at 1340 cm^{-1} corresponding to a breathing mode or κ-point photons of A_{1g} symmetry and a relatively weak G peak at 1605 cm^{-1} arise in GQDs, which is due to first order scattering of the E_{2g} photons caused by the in plane bond-stretching motion of pairs of C Sp^2 atoms.[20] Low D/G intensity ratio indicates a good crystalline structure but in case of GQDs I_D/I_G is always higher due to increased number of edges as the size becomes smaller in GQDs.[9] This GQDs showed a ratio I_D/I_G= 1.1. However, in case of GQDs there are two factors which contribute to the D band, one is due to lack of crystallinity and the other due to decrease in size. Due to smaller size of GQDs, indeed, the number of defect sites increases in the edges which contributes to the D band. Figure S 2 (a) represents the XPS analysis of the prepared GQDs where the C and O 1s peaks are seen in the survey spectrum with an atomic percentage ratio of 68.8 : 31.2 for C : O. Upon deconvolution of the C 1s peak (Figure S 2 (b)), 5 peaks arise due to graphitic C=C (284 eV), C-C (284.9 eV), C=O (286.5 eV), -C-O (288.9 eV) and -COOH (291.1eV) respectively.

A schematic for room temperature photo activity of a GQD device is presented in Figure 3 (a). For measuring the I-V responses, the GQD device was mounted on a cold finger and pumped overnight under a vacuum of ~ 10^{-5} Torr. I-V response with light off and light on was obtained using a laser line of λ= 658 nm at 60 mW power. The data is presented in Figure 3 (b). The linear I-V response with light off indicates an Ohmic contact. We also found low zero-bias photocurrent in our device, indicating no photovoltaic contribution due to barrier effects at the contacts. In other words, the photoconduction is attributed due to the photo carrier generation within the bulk of the GQD film.

We have also measured the dependence of photocurrent I_{ph} ($I_{ph} = I_{ill} - I_{dark}$) on laser intensity P under a wide range of laser intensities (5mW ≤ P ≤ 60wW). A non-linear dependence of I_{ph} on light intensity was observed. We found that I_{ph} shows a power dependence behavior $I_{ph} \sim P^{\gamma}$, where P is laser intensity with γ = 0.85 (Figure 3 c). The fractional power dependence of I_{ph} on laser intensity P is generally observed in amorphous or disordered semiconductor thin films and is attributed to the presence of a large number of trap states in these materials. In order to check the stability and the reliability of the photocurrent generated, the laser source was switched ON and OFF in roughly at a frequency ~ 1Hz with varying laser output equal to 60mW. This data is presented in Figure 3 (d).

We have also measured the dependence of I_{ph} with temperature (35 K < T < 285 K) by applying a DC bias of 10 V, under a constant illumination (λ= 658 nm, E= 1.8 eV) at 60 mW. The data is presented in Figure 4 (a). In Figure 4 (b) $\ln(I_{ph})$ plotted as a function of 1/T is presented. Where the data shows that depending on the measurement temperatures, two distinct regions for I_{ph} can be identified: Region I (T > ~ 100 K) and Region II (T < ~ 100 K).

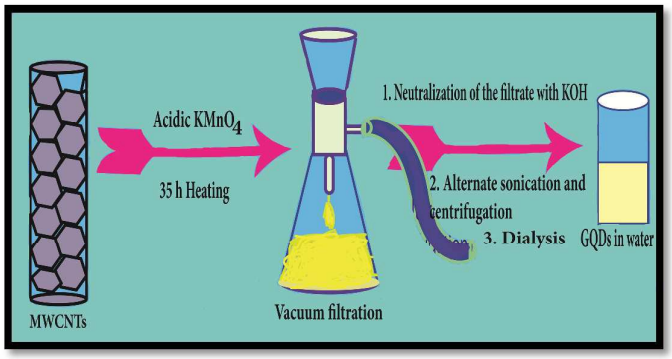

Figure 1: Schematic diagram of the experimental set up

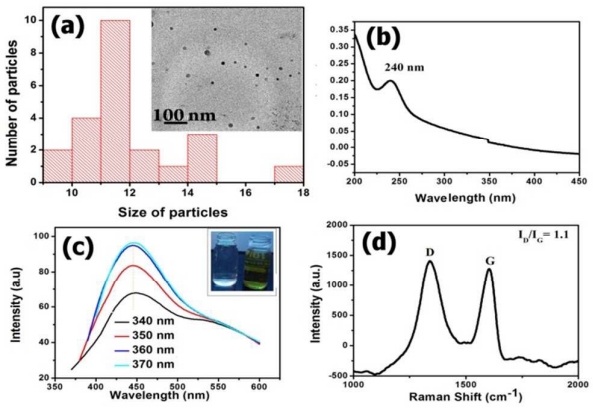

Figure 2: a: TEM image of 12 nm GQDs b: UV of GQDs in water c: Emission spectra of fluorescence and in inset the color of GQDs under UV lamp d: Raman shift

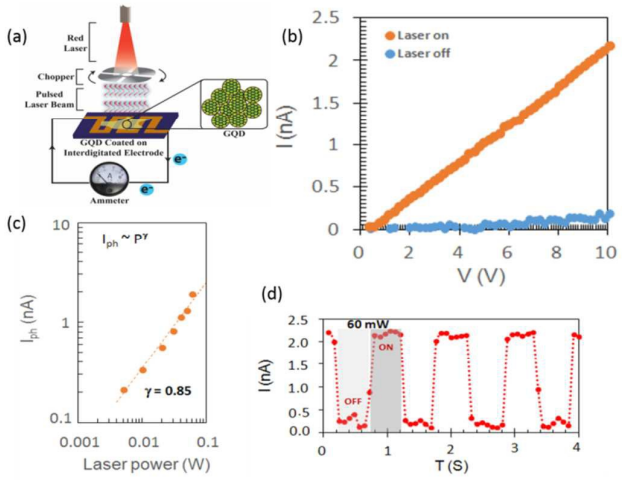

Figure 3.(a) Photocurrent measurement set up (b) Photocurrent with applied potential (c) Variation of photocurrent with incident laser power (dashed line is a fit with a power exponent 0.85) (d) ON-OFF switching of the GQD device with the laser ON-OFF.

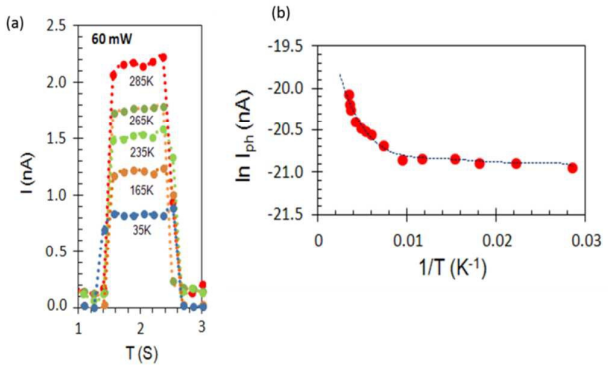

Figure 4.(a) Comparison of I_{ph} for few selected temperatures in GQD thin film is shown. (b) The temperature dependence of I_{ph} for the temperature range studied is presented. An increase photocurrent at higher temperatures is observed. At low temperatures I_{ph} was found to be constant. as well as higher value of photocurrent compared to dark current at lower temperatures is shown.

In region I, I_{ph} increases with increase in temperature (from ~ 100 K > T > 285 K). The photo response measured on the GQD's shows signatures of disordered film. In disordered materials presence of trap states between the valence and conduction band, plays an important role in the photo conduction mechanisms. In case of very few and discrete trap states (mostly found in materials without any disorder), the photocurrent is expected to be constant over a wide range of temperature. However, in case of highly disordered materials, a possibility of a continuous distribution of trap state might occur. In such cases, the nature of the distribution of the trap states, to a large extent controls the photo response under different conditions (for example, varying laser intensity or temperature). We believe that in the present case, at low temperature (T<100K) a large number of the trapped photo excited carriers have thermal energies much lower than the activation energies needed for them to contribute to the photocurrent generation phenomenon. However, as the temperature is increased (beyond 100K in this particular case), the trapped photo excited carriers gain enough thermal energy to overcome the trap barrier and contribute to the conduction process. This leads to an overall increase in the measured photocurrent. In the past, it has been shown for several photoactive disordered semiconductors that in the higher temperature region the photoconduction is carried through extended states and a result as the temperature increases the number of thermally generated carriers also increase which perhaps participate in the photoconduction process. Thus as the temperature is increased I_{ph} also increases. At sufficiently low temperatures (T ≤ 100 K), a constant I_{ph} is observed, indicating a constant photo carrier density in the device once the temperature reaches below ~100 K.

In conclusion we have shown that fluorescent graphene quantum dots can be easily obtained by using a simple chemical route of acid treatment of MWNTS. Our investigation also sheds light on the possible mechanism of photo conduction in these GQD films. Low temperature optical properties of thin films of these graphene quantum dots show that their optical properties follow a behavior similar to that of disordered photoactive materials. We believe that these investigations can lead to large scale production of quantum dots which can possibly be harnessed for several opto-electronic based applications.

This work has been supported by **IUSSTF** joint center on **"3D engineered electrodes for electrochemical energy storage"** through a grant number **22-2012/2013-14**. Authors thank Mr. A. Rathish Kumar and all other CIF staffs, CSIR-CECRI for their help rendered during the characterization of the samples. S.K acknowledges Mr. Joyashish Debgupta (NCL, Pune, India) and Dr. Deepak Kumar Pattanayak for their help during the execution of this project.

Notes and references

1 M. A. Sk, A. Ananthanarayanan, L. Huang, K. H. Lim and P. Chen, *J. Mater. Chem. C*, 2014, **2**, 6954–6960.

2 M. Bacon, S. J. Bradley and T. Nann, *Part. Part. Syst. Charact.*, 2014, **31**, 415–428.
3 S. H. Song, M.-H. Jang, J. Chung, S. H. Jin, B. H. Kim, S.-H. Hur, S. Yoo, Y.-H. Cho and S. Jeon, *Adv. Opt. Mater.*, 2014, **2**, 1016–1023.
4 A. K. Geim, *Sci.* , 2009, **324** , 1530–1534.
5 D. B. Shinde and V. K. Pillai, *Angew. Chem. Int. Ed. Engl.*, 2013, **52**, 2482–2485.
6 (a)L. Li, G. Wu, G. Yang, J. Peng, J. Zhao and J.-J. Zhu, *Nanoscale*, 2013, **5**, 4015–4039. (b) S. Kundu, R. M. Yadav, M.V. Shelke, T.N. Narayanan, R Vajtai, Pulickel M. Ajayan, and V. K. Pillai.; *Nanoscale*, 2015, **7**, 11515-11519.
7 J. Peng, W. Gao, B. K. Gupta, Z. Liu, R. Romero-Aburto, L. Ge, L. Song, L. B. Alemany, X. Zhan, G. Gao, S. A. Vithayathil, B. A. Kaipparettu, A. a Marti, T. Hayashi, J.-J. Zhu and P. M. Ajayan, *Nano Lett.*, 2012, **12**, 844–849.
8 R. Ye, C. Xiang, J. Lin, Z. Peng, K. Huang, Z. Yan, N. P. Cook, E. L. G. Samuel, C.-C. Hwang, G. Ruan, G. Ceriotti, A.-R. O. Raji, A. a Martí and J. M. Tour, *Nat. Commun.*, 2013, **4**, 1–6.
9 J. Kim and J. S. Suh, *ACS Nano*, 2014, **8**, 4190–4196.
10 Y. Shin, J. Lee, J. Yang, J. Park, K. Lee, S. Kim, Y. Park and H. Lee, *Small*, 2014, **10**, 866–870.
11 Z. Zhang, J. Zhang, N. Chen and L. Qu, *Energy Environ. Sci.*, 2012, **5**, 8869–8890.
12 C. O. Girit, J. C. Meyer, R. Erni, M. D. Rossell, C. Kisielowski, L. Yang, C.-H. Park, M. F. Crommie, M. L. Cohen, S. G. Louie and A. Zettl, *Science*, 2009, **323**, 1705–1708.
13 F. Schedin, a K. Geim, S. V Morozov, E. W. Hill, P. Blake, M. I. Katsnelson and K. S. Novoselov, *Nat. Mater.*, 2007, **6**, 652–5.
14 J. Shen, Y. Zhu, X. Yang and C. Li, *Chem. Commun. (Camb).*, 2012, **48**, 3686–3699.
15 H. Sun, L. Wu, W. Wei and X. Qu, *Mater. Today*, 2013, **16**, 433–442.
16 B. Y. Zhang, T. Liu, B. Meng, X. Li, G. Liang, X. Hu and Q. J. Wang, *Nat. Commun.*, 2013, **4**, 1811.
17 F. Xia, T. Mueller, Y.-M. Lin, A. Valdes-Garcia and P. Avouris, *Nat. Nanotechnol.*, 2009, **4**, 839–843.
18 G. Konstantatos, M. Badioli, L. Gaudreau, J. Osmond, M. Bernechea, F. P. Garcia de Arquer, F. Gatti and F. H. L. Koppens, *Nat. Nanotechnol.*, 2012, **7**, 363–368.
19 T. Mueller, F. Xia and P. Avouris, *Nat. Photonics*, 2010, **4**, 297–301.
20 G. Wang, X. Shen, J. Yao and J. Park, *Carbon N. Y.*, 2009, **47**, 2049–2053.